Demonstration of a Photonically Controlled RF Phase Shifter

Sang-Shin Lee, Anand H. Udupa, Hernan Erlig, Hua Zhang, Yian Chang, Cheng Zhang, Daniel H. Chang, Daipayan Bhattacharya, Boris Tsap, William H. Steier, Larry R. Dalton, and Harold R. Fetterman

***Abstract*— Integrated photonic radio frequency (RF) phase shifters with dc voltage control have been realized using a nested dual Mach–Zehnder modulator configuration in a new nonlinear optical polymer, CLD2-ISX. These modulators have a V_π of 10.8 V and exhibit excellent frequency performance measured up to 20 GHz. A near linear phase shift exceeding 108° was obtained for a 16-GHz microwave signal by tuning the dc control voltage over a 7.8-V range. It is expected that these integrated polymer phase shifters will find widespread applications in new types of lightweight optically controlled phased array systems.**

***Index Terms*— Nested Mach–Zehnder modulators, nonlinear optical polymers, photonic RF phase shifters, traveling-wave polymer modulators.**

I. Introduction

PHASED arrays are playing an increasingly significant role in space-based applications. However, a practical implementation of arrays with thousands of elements is limited by the complexity of the feed structures and active phase-shifting elements. The use of integrated photonics for the realization of phased array beam-forming is of much interest due to benefits like low cost, lightweight, and low power consumption [1], [2]. One of the key components of such an integrated approach is a photonic radio frequency (RF) phase shifter that can provide an accurate and easily controllable phase shift.

Various architectures for constructing photonic RF phase shifters have been realized on $LiNbO_3$ [3]–[5]. In this letter, we report the design, fabrication, and performance of a voltage-controlled RF phase shifter based on a new EO polymer, CLD2-ISX. We have, in the past, demonstrated the high-frequency capabilities of our polymer traveling wave modulators that arise from a near perfect velocity match between the optical and microwave fields [6]. Since the phase shifters have a similar traveling wave configuration, they are expected to perform well up to frequencies exceeding 100 GHz.

Manuscript received March 30, 1999; revised June 23, 1999. This work was supported under grants from the Air Force Office of Scientific Research (AFOSR) and the Office of Naval Research (ONR).

S.-S. Lee is with LG Corporate Institute of Technology, Seoul, South Korea.

A. H. Udupa, D. H. Chang, D. Bhattacharya, and H. R. Fetterman are with the Department of Electrical Engineering, University of California, Los Angeles, CA 90095 USA.

H. Erlig, Y. Chang, and B. Tsap are with Pacific Wave Industries, Los Angeles, CA 90024 USA.

H. Zhang, C. Zhang, W. H. Steier, and L. R. Dalton are with the Department of Electrical Engineering and Chemistry, University of Southern California, Los Angeles, CA 90089 USA.

Publisher Item Identifier S 1051-8207(99)07583-2.

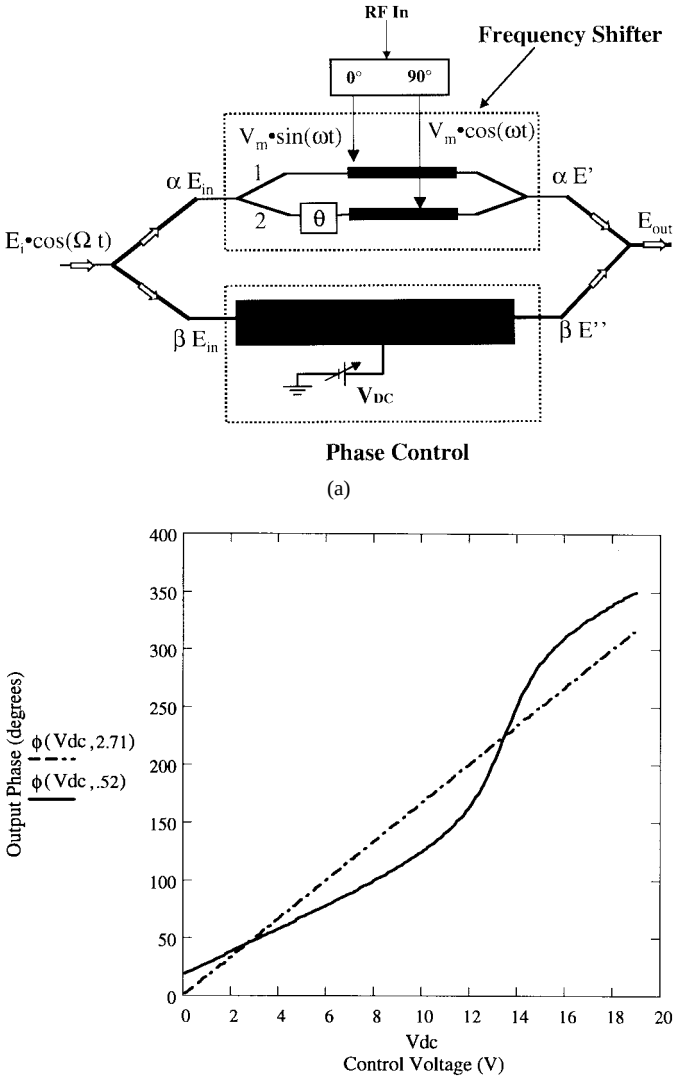

Fig. 1. (a) Schematic of the RF phase shifter. Ω and ω are the optical and microwave frequencies, respectively. (b) Calculated phase shift characteristics as a function of control dc voltage. The solid line corresponds to the case of $\Delta = 0.52$ whereas the dotted line corresponds to $\Delta = 2.71$.

II. Theory

The basic configuration of our RF phase shifter is shown in Fig. 1(a). The optical input is a laser beam described by the field $E_{\mathrm{in}} = E_i \cdot \cos(\Omega t)$. This beam is split in the ratio $\alpha : \beta$ at the first Y-junction and equally at the second Y-junction. The electrodes of the arms 1 and 2 are driven with the in-phase

and quadrature components derived from the same microwave source. The RF driving frequency and amplitude are denoted by ω and V_m, respectively. An additional optical phase shift θ is introduced in arm 2 using a dc bias. If θ is chosen to be 90°, a single-sideband (SSB) output is obtained at frequency $(\Omega+\omega)$ [5] at the output of the embedded Mach–Zehnder and the following expressions for the fields $\alpha E'$ and $\beta E''$ can be derived:

$$\alpha E' = \alpha \frac{E_i}{2}\{\cos(\Omega t + \Delta \sin \omega t) + \cos(\Omega t + \pi/2 + \Delta \cos \omega t)\} \quad (1)$$

$$\beta E'' = \beta E_i \cos(\Omega t + \phi_{\mathrm{DC}}) \quad (2)$$

where $\Delta = \pi \cdot V_m/V_\pi$, $\phi_{\mathrm{DC}} = \pi \cdot V_{\mathrm{DC}}/V_\pi$, and V_{DC} is the voltage on the dc control electrode. V_π is the half-wave voltage corresponding to the section of the EO polymer under the microstrip line.

In the case that $\alpha = \beta = 1/\sqrt{2}$ the total output electric field is given by

$$E_{\mathrm{out}} = \tfrac{1}{2}(E' + E'') = \frac{E_i}{2}\left\{\frac{1}{2}[\cos(\Omega t + \Delta \sin \omega t) - \sin(\Omega t + \Delta \cos \omega t)] + \cos(\Omega t + \phi_{\mathrm{DC}})\right\}. \quad (3)$$

The following terms of the total intensity will contribute to the intensity at the modulation frequency, ω; these are

$$I(\omega) \propto \frac{E_i^2}{16}[2\cos(\Delta \sin \omega t - \phi_{\mathrm{DC}}) - 2\sin(\Delta \cos \omega t - \phi_{\mathrm{DC}}) + \sin(\Delta \sin \omega t - \Delta \cos \omega t)]. \quad (4a)$$

It should be noted from (4a) that these terms also contribute to the dc and harmonics of ω in the total intensity. From (4a) the resulting expression for the optical intensity at the modulation frequency is

$$I_\omega = \frac{E_i^2}{16}\left\{\left(\sqrt{2}\,J_1\left(\sqrt{2}\,\Delta\right) + 4J_1(\Delta)\sin\phi_{\mathrm{DC}}\right) \cdot \sin \omega t - \left(\sqrt{2}J_1\left(\sqrt{2}\,\Delta\right) + 4J_1(\Delta)\cos\phi_{\mathrm{DC}}\right)\cos \omega t\right\} \quad (4b)$$

where J_1 is the first-order Bessel function. Note that the intensity at the modulation frequency is solely dependent on the first-order Bessel function. For a choice of $\Delta = 2.71$ we find that $J_1(\sqrt{2}\,\Delta) = 0$. Under these conditions equation (4b) reduces to

$$I_\omega = \frac{E_i^2}{4} J_1(2.71) \cdot \cos(\omega t + \phi_{\mathrm{DC}} + \pi). \quad (5)$$

Thus for $V_m^{\mathrm{lin}} = 0.86V_\pi$, which corresponds to $\Delta = 2.71$, the phase shift is linear with respect to the control voltage as seen in Fig. 1(b). However, for a V_π of 10.8 V this condition requires a sizable microwave signal. Therefore, for the results reported in this letter we operate within the realm of the small-signal approximation. Under this condition (4b) reduces to

$$I_\omega = \frac{E_i^2}{16}\Delta \cdot A_{\mathrm{DC}} \cdot \cos(\omega t + \chi_{\mathrm{DC}} + \pi) \quad (6)$$

where $\chi_{\mathrm{DC}} = \tan^{-1}[(1 + 2 \cdot \sin\phi_{\mathrm{DC}})/(1 + 2 \cdot \cos\phi_{\mathrm{DC}})]$, $A_{\mathrm{DC}} = \sqrt{(1 + 2 \cdot \sin\phi_{\mathrm{DC}})^2 + (1 + 2 \cdot \cos\phi_{\mathrm{DC}})^2}$, and where we have assumed that $J_1(\Delta) \approx \Delta/2$. Fig. 1(b) also shows the transfer characteristics for the case that $\Delta = 0.52$, which is similar to the values generated for the experiment. Note there is a range of nearly 100° over which the microwave phase varies nearly linearly with respect to control dc voltage.

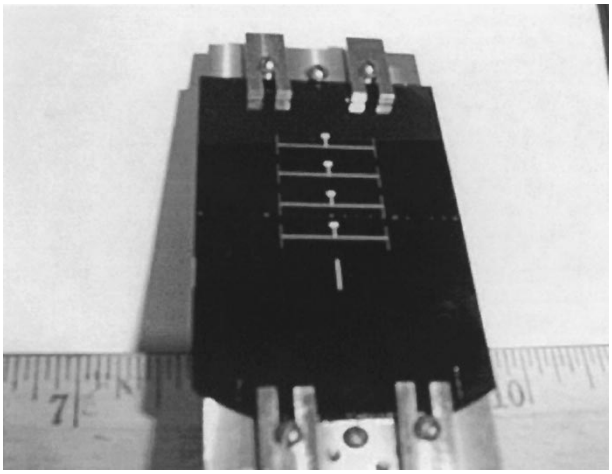

Fig. 2. Photograph of the RF phase shifter. The above chip consists of four individual integrated RF phase shifters.

III. Device Fabrication

A silicon wafer was used as a mechanical support, on which the lower ground electrode consisting of chromium and gold was deposited. The lower cladding and active polymer layer were spin coated and the active polymer corona poled. Optical rib waveguides were defined on the active polymer using reactive ion etching. The upper cladding was spun on, and 4-μm-thick gold electrodes patterned [7]. The cladding layers used in fabrication were made of UV-15, a UV curable epoxy. The active chromophore used was CLD2-ISX [8], which was crosslinked into a polyurethane matrix. This chromophore exhibits a high nonlinearity r_{33} equal to 37 pm/V at 1060 nm. It has a high decomposition temperature of 194.4 °C leading to long-term thermal stability. CLD2-ISX has an absorption maximum at 570 nm and introduces no additional optical loss at 1310 nm. A photograph of the fabricated device is shown in Fig. 2.

IV. Experimental Results

Using a low-frequency measurement technique, we measured the V_π of the phase shifter to be 10.8 V. This value corresponds to the case where modulation is applied to arm 1 only. To study the high-frequency performance of the constituent modulators, the microstrip electrodes of arms 1 and 2 were independently driven at 16 GHz and the modulation directly monitored on a HP 8592A spectrum analyzer.

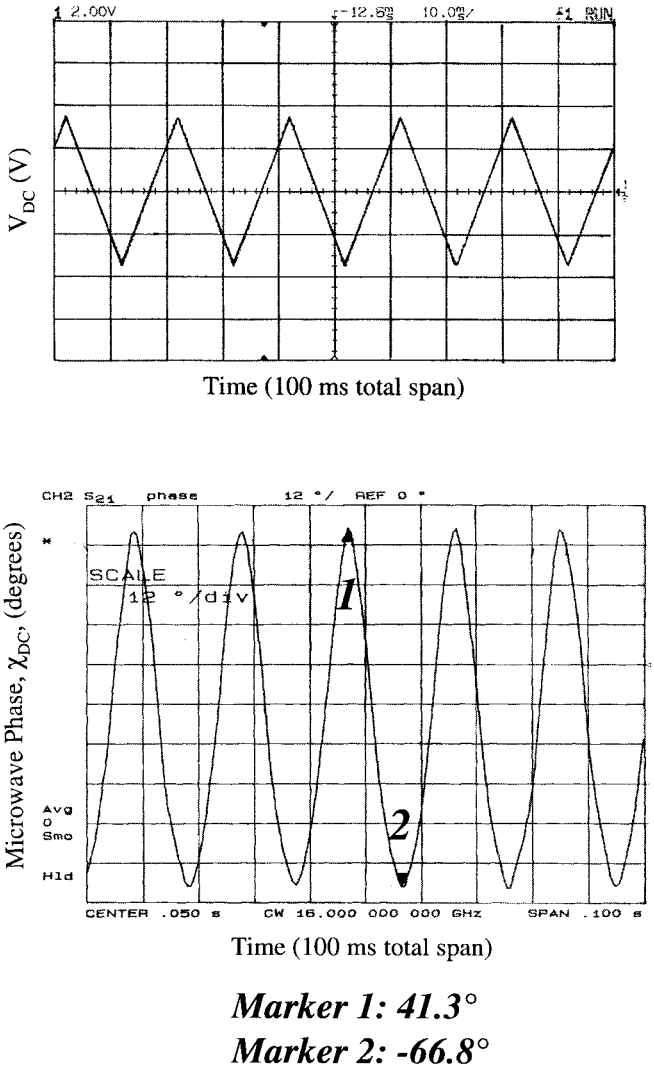

Fig. 3. The bottom plot shows the phase shift variation as seen on the network analyzer for a 50-Hz triangular waveform applied to the dc electrode (shown in the top plot). As can be seen, the phase changes by 108° for a peak-to-peak control voltage of 7.8 V.

The modulation signals from the two arms were equal to within 1 dB. This confirms that the inner Mach–Zehnder is well-balanced, a criterion that is important for linear phase characteristics.

The phase shifter transfer characteristics were measured as follows. Port 1 of a HP 8510 network analyzer was used as the microwave source at 16 GHz. A 3-dB power splitter was used to produce the two driving arms. Their lengths were set to be 90° out of phase with each other at the feeds. Coplanar probes were used to launch the signals onto the microstrip electrodes. The driving power on each electrode was set to 15 dBm (approximately small signal). A bias tee on arm 2 provided the dc bias for the 90° optical phase shift. Light from a Nd:YAG laser ($\lambda = 1310$ nm) was butt-coupled to the optical waveguide endface using a single-mode PM fiber. Optical coupling loss from the fiber to the rib waveguide was found to be high, but the use of a lensed fiber resulted in a 3-dB improvement. The modulated light was registered by a photodetector, whose output was sent to port 2 of the network analyzer for phase comparison with the source. A HP function generator was used to drive the dc control pad via a dc probe with a 50-Hz triangular wave.

The phase shift characteristics for a triangular wave of peak-to-peak voltage of 7.8 V is shown in Fig. 3. In this case a phase shift exceeding 108° was obtained. It can be seen that the phase shift versus control voltage characteristic is relatively linear with a slope that corresponds to 13.9°/V. A phase shift up to 360° was also obtained by tuning the control voltage from 0 to 25 V, with a compromise on linearity. A 6-dB change in microwave output power was observed corresponding to a microwave phase shift of 90°; this is as expected from (6).

V. Conclusion

In the past, the high-speed potentials and impressive nonlinearities of EO polymer systems have been demonstrated. The successful fabrication of the phase shifter further illustrates the maturity of the polymer waveguide technology and the possibility of realizing other novel configurations of photonic integrated devices. In conclusion, CLD2-ISX, a new EO polymer with high nonlinearity and low loss has been used to fabricate integrated RF phase shifters. These devices have low V_π and exhibit excellent modulation characteristics tested up to 20 GHz. The phase of the input microwave can be shifted over 108° by tuning the dc control voltage over a 7.8-V range. In this tuning range the microwave phase varied nearly linearly with respect to the dc control voltage. These devices are expected to have widespread applications in future phased array radar and antenna systems that utilize integrated photonics. Use of polymer materials for these structures makes it possible to realize complex devices and even arrays.

References

[1] G. L. Tangonan, "Optoelectronics for radar applications," in *Optical Technology for Microwave Applications IV, Proc. SPIE,* Mar. 1989, vol. 1102, pp. 34–38.

[2] M. Tamburrini, M. Parent, L. Goldberg, and D. Stillwell, "Optical feed for a phased array microwave antenna," *Electron. Lett.*, vol. 23, no. 13, pp. 680–681, June 1987.

[3] Y. Kamiya, W. Chujo, Y. Koji, K. Matsumoto, M. Izutsu, and T. Sueta, "Fiber optic array antenna using optical waveguide structures," in *IEEE Int. Symp. Dig., Antennas and Propagation,* May 1990, vol. 2072, pp. 774–777.

[4] J. F. Coward, T. K. Yee, C. H. Chalfant, and P. H. Chang, "A photonic integrated-optic RF phase shifter for phased array antenna beam-forming applications," *IEEE J. Lightwave Technol.*, vol. 11, pp. 2201–2205, Dec. 1993.

[5] D. R. Jez, K. J. Cearns, and P. E. Jessop, "Optical waveguide components for beam forming in phased array antennas," *Microw. Opt. Technol. Lett.*, vol. 15, no. 1, pp. 46–49, May 1997.

[6] D. Chen, H. R. Fetterman, A. Chen, W. H. Steier, L. R. Dalton, W. Wang, and Y. Shi, "Demonstration of 110 GHz electro-optic polymer modulators," *Appl. Phys. Lett.*, vol. 70, no. 25, pp. 3335–3337, June 1997.

[7] D. Chen, D. Bhattacharya, A. Udupa, B. Tsap, H. R. Fetterman, A. Chen, S. S. Lee, J. Chen, W. H. Steier, and L. R. Dalton, "High frequency polymer modulators with integrated finline transitions and low V_π," *IEEE Photon. Technol. Lett.*, vol. 11, pp. 54–56, Jan. 1999.

[8] C. Zhang, C. Wang, L. R. Dalton, G. Sun, H. Zhang, and W. H. Steier, "Investigation on new polyurethanes and incorporation of a soluble high $\mu\beta$ chromophore for electro-optic applications," *Polym. Preprints*, vol. 40, no. 1, pp. 51–52, Jan. 1999.